Inhibition of IκB Kinase-β and Anticancer Activities of Novel Chalcone Adamantyl Arotinoids

Paula Lorenzo,[†] Rosana Alvarez,[†] Maria A. Ortiz,[‡] Susana Alvarez,[†] F. Javier Piedrafita,*[,‡] and Ángel R. de Lera*[,†]

Departamento de Química Orgánica, Universidade de Vigo, Lagoas-Marcosende, 36310 Vigo, Spain, and Sidney Kimmel Cancer Center, 10905 Road to the Cure, San Diego, California 92121

Received March 14, 2008

On the basis of the observations that chalcone **7** (MX781) and some related adamantyl arotinoids (AdAr**s**) inhibit IκBα kinase β (IKKβ) activity, inhibit cell growth, and induce apoptosis in cancer cells, a new series of AdArs structurally related to **7** have been designed and synthesized. Modifications were intended to reduce or eliminate RAR activity, and we evaluated the effect of the novel analogues of **7** on IKKβ activity and proliferation of a variety of cancer cell lines (leukemia, Jurkat; prostate, PC-3; breast carcinomas, T47D, MDA-MB-468). Consistent with the design principles, the biological activities of these AdArs do not appear to be RAR-mediated, since most analogues are unable to activate RAR-mediated transactivation and exhibit significantly diminished antagonist activity. All compounds are capable of inducing apoptosis in Jurkat cells, as demonstrated by elevated DEVDase activity and externalization of phosphatidylserine. Several of the analogues elicit stronger growth inhibitory activity against prostate (PC-3) and breast (MDA-MB-468) carcinoma cells, which contain elevated basal IKK activity; this antiproliferative activity correlates with increased inhibition of recombinant IKKβ in vitro, suggesting that the anticancer activities of these AdArs might be related to the inhibition of IKK/NFκB signaling.

Introduction

The retinoids, natural and synthetic analogues of retinol (vitamin A), are key regulators of many biological events including cell growth and differentiation, development, homeostasis, and carcinogenesis.[1−3] Most of these biological functions are mediated by the complexes obtained after binding of ligands to the retinoic acid receptors (RARs,[a] subtypes α, β, and γ) and retinoid X receptors (RXRs, subtypes α, β, and γ), which are members of the nuclear receptor superfamily.[4−6] Structural information is available on both unbound apo- and holoretinoid receptors bound to a variety of ligands,[7] which has facilitated the design of more potent modulators of retinoid receptor action such as antagonists, inverse agonists, and agonists selective for a particular RAR subtype,[8] as well as RXR-selective retinoids or rexinoids. Some of these selective retinoids or rexinoids show enhanced antiproliferative activity against cancer cells, which correlates with their ability to induce cell differentiation, growth arrest, and apoptosis.[9] The highly promising potential of vitamin A and its derivatives as cancer preventive and chemotherapeutic agents has, however, not yet been fully realized because of the toxic side effects observed, which somehow limit their therapeutic use.[10]

A subgroup of retinoids, termed collectively atypical retinoids or retinoid related molecules (RRMs),[10,11] does not fit into the conventional concept of retinoid action. Although inspired on the structure of classical retinoids, either they do not bind to the retinoid receptors or their strong growth inhibitory or apoptogenic activities do not appear to be retinoid receptor-mediated. Anhydroretinol **1**, 4-hydrophenylretinamide **2**, and **3** (6-[(3-adamant-1-yl)-4-hydroxy-phenyl]-2-naphthoic acid, CD437, also called AHPN) are classical examples of RRMs (see Figure 1) that induce growth arrest and apoptosis in a variety of cancer cell lines. Within this class, the adamantyl arotinoids (AdArs), of which **3** is the prototype lead compound, have been the most thoroughly studied. Novel derivatives of **3** (including 5-Cl-AHPN **4** and 3-Cl-AHPC **6**; see Figure 1) have been obtained that preserve apoptotic activity but lack RAR transactivation activity.[12−14]

The mechanism of RRM-mediated cell death, in particular the induced apoptosis by **3**, has been investigated by numerous laboratories and seems to be largely dependent on cell type. RRMs have been shown to inhibit cell growth by caspase-dependent and independent mechanisms [15−17] and induce apoptosis via the intrinsic pathway,[18,19] although activation of the death receptor-mediated extrinsic pathway has also been demonstrated in some cases.[20] Even though the majority of the RRMs bind and activate the nuclear RARs, they seem to induce apoptosis independently of RARs,[11] most likely by binding to and modulating the activity of other cellular receptors yet to be identified. Compound **3** and other RRM analogues induced a strong and sustained activation of cJun N-terminal kinase (JNK) and p38 stress kinases in several cancer cell lines independently of caspase activity[21] (and our unpublished observations). In Jurkat T cells, pharmacological inhibition of both JNK and p38 MAPK prevented the release of cytochrome *c* and subsequent induction of apoptosis.[21] Other groups have reported contradictory results with different MAPK inhibitors and various cancer cell lines. Thus, inhibition of p38 reduced the apoptosis induced by **3** in ovarian carcinoma cells,[22] whereas inhibition of JNK partially prevented the induction of cell death in AML cells by **6**.[23] In contrast, several MAPK inhibitors had no effect on RRM activity in various leukemia cells.[13,24,25] In addition to inducing MAPK activity, RAR antagonist **7** ((*E*)-4-{3-[(3-adamant-1-yl)-4-(2-methoxyethoxymethoxy)-phenyl]-3-oxoprop-1-en-1-yl}benzoic acid, MX781) and RAR agonist **8** (CD2325) substantially inhibited the activity of IKK isolated from TNFα-stimulated HeLa cells, although only the antagonist displayed

* To whom correspondence should be addressed. For F.J.P.: phone, +1-858-410-4188; fax, +1-858-450-3251; e-mail, jpiedrafita@skcc.org. For Á.R.d.L.: phone, +34-986-812316; fax, +34-986-811940; e-mail, qolera@uvigo.es.

[†] Universidade de Vigo.

[‡] Sidney Kimmel Cancer Center.

[a] Abbreviations: AdArs, adamantyl arotinoids; ATRA: all-*trans*-retinoic acid; IKK, IκB kinase; JNK, cJun N-terminal kinase; PI, propidium iodine; RAR, retinoic acid receptor; RRMs, retinoid-related molecules; RXR, retinoid X receptor.

10.1021/jm800285f CCC: $40.75
Published on Web 08/14/2008

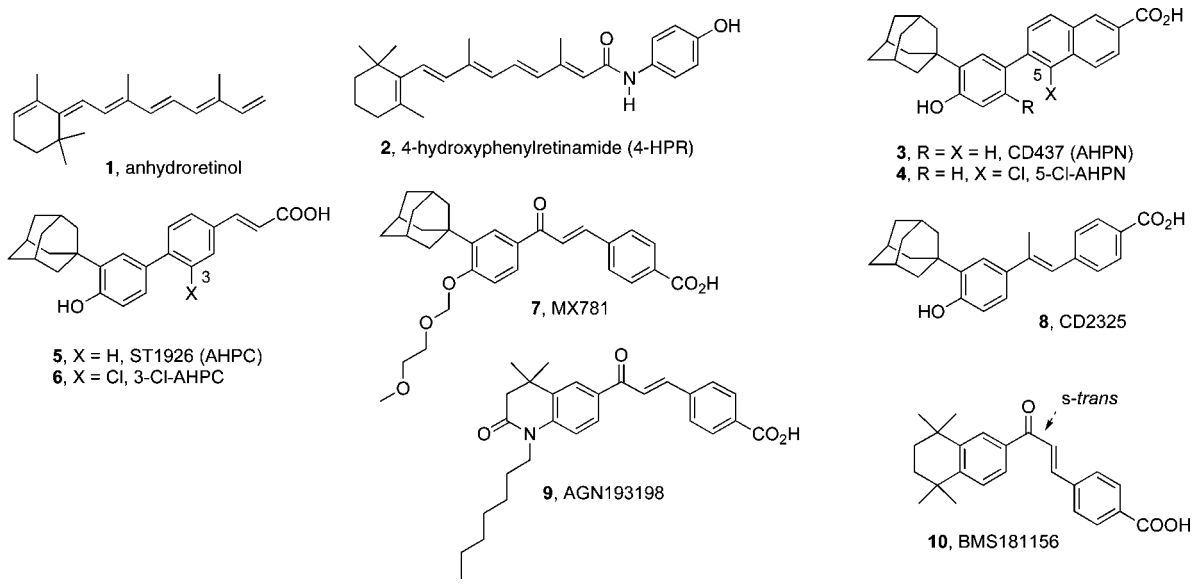

Figure 1. Structure of selected RRMs including those with chalcone and adamantyl groups. A chalcone retinoid (**10**) in its RARγ-bound s-trans conformation is also shown.

effective and consistent inhibition of IKK/NFκB signals in a number of cancer cell lines.[26] Targeting IKK/NFκB pathways by means of kinase dead IKK mutants or a nonphosphorylable form of IκBα was sufficient to induce cell death, further supporting an important role for IKK and NFκB activity in cell survival by inhibiting apoptosis.[27−29] Our observations contrast with recent reports showing that **3** and **6** induced cell death via activation of NFκB in prostate and breast carcinoma cells.[30,31]

The scarcity of SAR studies on AdArs,[32] focusing primarily on binding to and transactivation through the RAR subtypes, precludes obtaining insights concerning the structural determinants that could mediate their anticancer activity. It is quite puzzling that **7** is the only AdAr known to significantly inhibit TNFα-mediated activation of IKK in cell-based assays.[26] The presence of both the chalcone and the adamantyl groups might be responsible for this profile, although each of these substructures is also present in other RRMs that show different biological profiling (Figure 1). For example, **9** (AGN193198) is a novel RAR antagonist that induces apoptosis with IC_{50} at nanomolar concentrations,[33] although its effect on IKK activity has not been reported. Compound **9** exhibits structural similarities with **7**, with a central chalcone and a long alkyl chain (the *N*-heptyl substituent) that resembles the acetal OMEM side chain of **7**. However, **9** lacks the adamantyl group, which could be considered partly responsible for the binding of **7** to IKK. Nevertheless, it is clear that the presence of this group is not sufficient given the fact that several related AdArs do not efficiently inhibit IKK in vitro or in intact cells. [26]

Given that IKK has been validated as a cancer therapeutic target by means of pharmacological and genetic inhibitors[34] and apoptotic AdArs can inhibit IKK in vitro and in cell assays,[26] we set out to synthesize a series of derivatives of **7** and examine their activities as IKK inhibitors to gain information on the structural determinants of this novel antikinase activity of AdArs. As a general objective, the designed AdArs should have reduced binding to the RARs and/or exhibit RAR antagonist profile. Comparative structural analysis suggests that the OMEM group of **7** or the *N*-heptyl substituent of **9** might be responsible for the RAR-antagonistic effects. The large substituent would displace the helix H12 from its agonist conformation and preclude binding of coactivators, in keeping with the classical mechanism of nuclear receptor antagonistic action.[35] However, the flexibility of the chalcone function in both **7** and **9** might counteract the effect to a certain degree. In fact, retinoid agonist **10** (BMS181156, Figure 1), which shares the chalcone function, adopts an s-trans conformation of the chalcone C(O)−C=C bond when bound to the RARγ receptor, as shown in the crystal structure of the complex.[36] We therefore planned to further distort the planarity around the chalcone unit of **7**, reduce its conformational flexibility, and disfavor the s-trans conformation by incorporating an additional substituent ortho to the carbonyl group (i.e., OR in **11**, Scheme 1), an approach complementary to the one described for **4** and **6** relative to the parent system.[12,14]

We report herein the synthesis of novel analogues of chalcone **7** (**11**, **24**) along with their biological characterization. Some of these AdArs surpass the lead compound in the inhibition of cell growth of several cancer cell lines, including leukemia, prostate, and estrogen-dependent and independent breast cancer cell lines. Because RAR transactivation was not detected, the antiproliferative activity of the novel AdArs must be independent of the activation of the retinoid receptors. Since the inhibition of recombinant IKKβ by several analogues is higher than that exhibited by **7** and correlates with increased growth inhibitory and apoptotic activities, it is possible that this antikinase activity of the analogues might be partially involved in their anticancer effect on cell lines that express high levels of basal IKK.

Synthesis

Preserving the location of the adamantyl and OMEM substituents of the parent structure, derivatives of **7** having alkyl chains of increasing length attached to the phenol vicinal to the chalcone unit were designed and synthesized as shown in Scheme 1. Additionally ethers incorporating unsaturated (allyl, propargyl) or aryl substituents were included and prepared using the same strategy. The Claisen−Schmidt condensation of methyl 4-formylbenzoate **23** and the ortho-substituted acetophenone derivative **22** was selected as the key step for the convergent construction of the chalcone functionality of the analogues substituted with hydroxy and alkoxy groups at the $C_{2'}$ position (structures **24** and **11**, Scheme 1).

The previously described[32] Friedel−Crafts-type alkylation of 2,4-dihydroxybenzaldehyde **14** and adamantan-1-ol **15** using sulfuric acid as catalyst was quite capricious in our hands, and

Scheme 1[a]

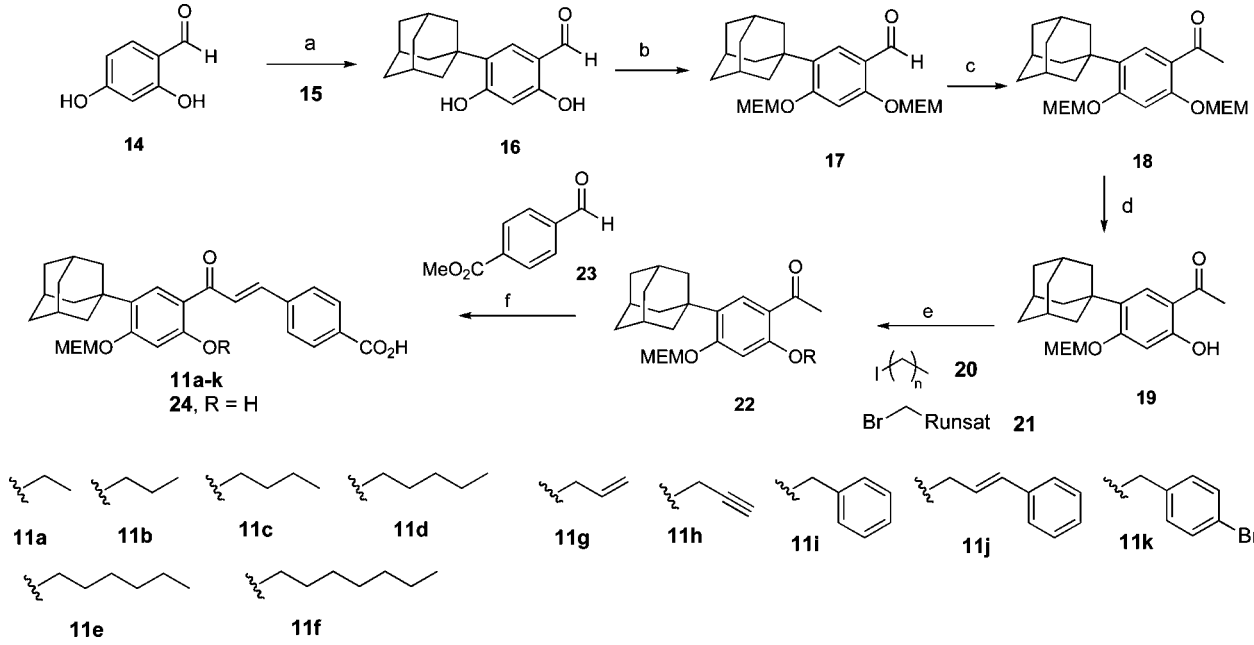

[a] Reagents and reaction conditions: (a) adamant-1-ol **15**, H_2SO_4, CH_2Cl_2, ultrasounds, 50 °C, 16 h (80%); (b) NaH, MEMCl, DMF, 25 °C, 19 h (98%); (c) (i) MeLi, Et_2O, 0 °C, 1.5 h; (ii) CrO_3/Py, CH_2Cl_2, 25 °C, 3 h (74%); (d) BCl_3, CH_2Cl_2, −78 °C, 18 h (74%); (e) HNa, DMF, 0 °C; then R−X **20** and **21**, 25 °C (59−95%); (f) NaOH, MeOH, 70 °C (22−58%).

the yields were highly variable (but not greater than 24%). Fortunately, the ultrasound irradiation of the heterogeneous mixture allowed the reaction to reach completion and improve performance (80% yield of **16**). This was followed by exhaustive phenol protection by treatment of **16** with NaH in DMF at 0 °C followed by trapping with MEMCl to afford **17** in 98% yield. The corresponding acetophenone **18** was acquired by addition of MeLi at 0 °C to **17** and oxidation of the secondary benzyl alcohol with CrO_3/pyridine in CH_2Cl_2 (74% combined yield, Scheme 1).[37]

Selective deprotection[32] of the C_2 phenol of **18** was achieved in 74% yield using 1 equiv of BCl_3 in CH_2Cl_2 at −78 °C. This outcome is presumably due to the coordinating ability of the vicinal ketone and the more hindered nature of the OMEM group at the alternative C_4 position. The same method described above for phenol protection was selected for the alkylation of **19** with alkyl (**20a**−**f**), allyl (**21g**,**j**), propargyl (**21h**), or benzyl halides (**21i, 21k**), reactions that took place in moderate to good yields (59−95%).

For the preparation of chalcones **11** and **24**, ketones **22** and **19**, respectively, were treated with methyl 4-formylbenzoate **23** using the classical Claisen−Schmidt condensation conditions described for the parent system (NaOH in MeOH at 70 °C).[38] The basic reaction conditions induced the saponification of the esters, and therefore, the desired carboxylic acids were obtained as final products. The yield decreased steadily upon increasing the length of the alkyl chain, and **20f** was unreactive. Likewise, halogenated benzylethers exhibited low reactivity, and **11k** (3.3% yield) was not used in the biological assays.

Biology

RAR Transactivation Profile. We first evaluated the RAR transactivation activity of the chalcones using CV-1 cells expressing Gal4-RAR fusion proteins following transient transfection of the corresponding expression vectors. Figure 2A illustrates that none of the compounds were capable of enhancing RAR-driven luciferase activity when tested alone. In contrast, when cells were stimulated with 1 μM all-*trans*-retinoic acid (ATRA), strong induction of luciferase activity was seen, in particular with the RARα fusion protein. We then examined the antagonistic activity of the chalcone analogues. CV-1 cells transfected with Gal4-RARα, RARβ, or RARγ were stimulated with 0.2 μM ATRA alone or together with 2 μM AdArs, a 10-fold molar excess of the candidate antagonists. For comparison, the antagonist activity of **7** and pan-inhibitor UVI2024 (BMS204493)[39] was also tested. Figure 2B illustrates that UVI2024 was a robust inhibitor of all three RARs whereas **7** strongly inhibited RARα. The inhibition of RARβ and RARγ mediated by **7** was substantially lower but still significant (30−40%). Among the analogues, **24** was a slightly better inhibitor of RARα than **7**, while it inhibited RARβ and RARγ with similar potency as **7**. The 2-ethoxy substitution in **11a** decreased RAR antagonist activity, and increasing the length of the alkyl chain substituent gradually eliminated the RAR antagonistic activity to almost completion in **11e**. Other allyl, propargyl, and aryl substitutions in position $C_{2'}$ similarly hindered RAR antagonistic activity (Figure 2B). Of note, **11h** inhibited RARα but not RARγ, whereas **11g** slightly inhibited RARγ and RARα but not RARβ. In general, a stronger inhibition of RARα was seen in the presence of the AdArs and only modest inhibition of RARβ was detected, which could be explained by the higher affinity of RARβ and RARγ for their natural ligand ATRA. None of the synthesized analogues activated RXRα-driven luciferase activity or inhibited 9-*cis*-retinoic acid or LGD1069-mediated activation of RXR (data not shown).

Anticancer Activity of the AdArs. To evaluate the antiproliferative activity of the novel analogues, we first tested their effect on the RRM-sensitive Jurkat T leukemia cell line using a MTT colorimetric assay. With the exception of phenol **24**, all other compounds elicited stronger antiproliferative activity compared to parent **7**. Compound **7** inhibited growth of Jurkat cells with an IC_{50} of 1.20 μM, whereas **11c** and **11i** were almost 4 times more active with IC_{50} values of 0.38 and 0.35 μM,

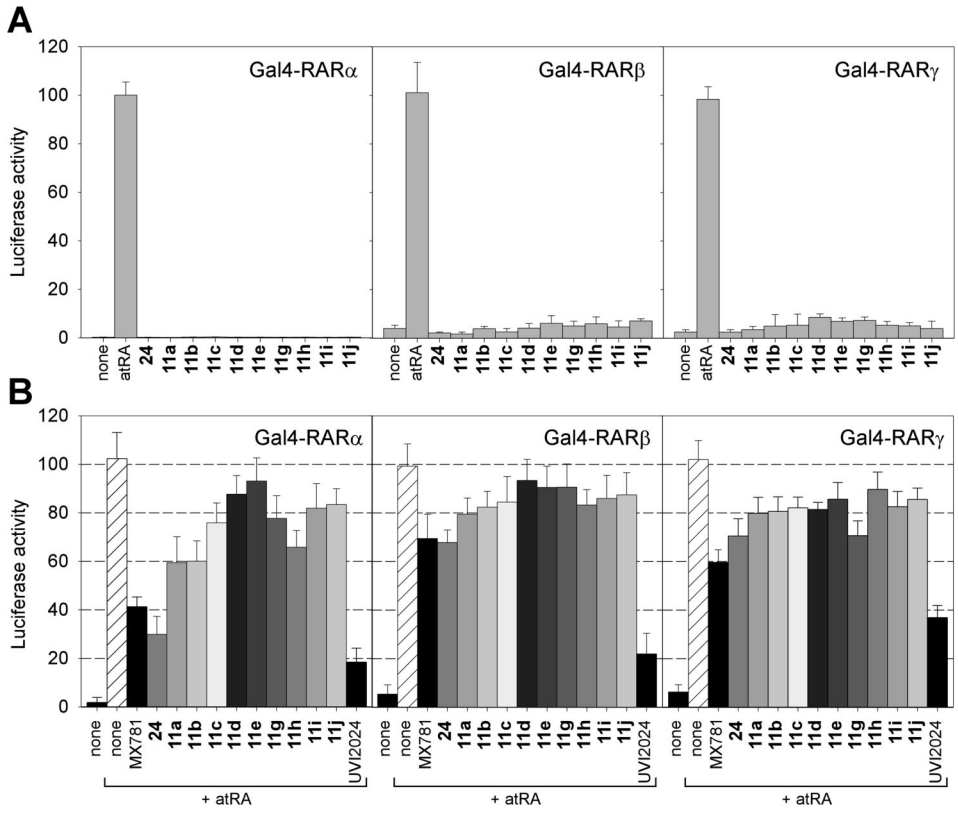

Figure 2. RAR transactivation profile of the novel AdAr s. CV-1 cells were cotransfected with 100 ng of UAS-luciferase reporter, 25 ng of β-galactosidase, and 10 ng of Gal4-RAR/RXR expression vectors. Sixteen hours after transfection, cells were treated with 1 μM ATRA (atRA) or 2 μM of the indicated compounds (A). To evaluate the antagonistic activity of the analogues, cells were stimulated with 0.2 μM ATRA alone (hatched column) or together with 2 μM of the indicated AdAr s (in gray scale) (B). Luciferase and β-galactosidase activities were measured after 6 (RARα,β) or 20 h (RARγ) of AdAr stimulation following standard procedures. Normalized luciferase activity was calculated and referenced to percentage of maximum activity obtained in the presence of ATRA. The average ± SD of at least two experiments performed in triplicate is shown.

Table 1. Inhibition of Cancer Cell Growth by AdAr s[a]

	Jurkat	PC-3	T-47D	MB-468
7	1.20 ± 0.12	1.48 ± 0.40	3.27 ± 0.17	2.11 ± 0.21
24	1.89 ± 0.14	2.51 ± 0.17	8.00 ± 0.40	6.08 ± 0.42
11a	1.14 ± 0.14	1.86 ± 0.44	5.01 ± 0.09	1.79 ± 0.29
11b	0.80 ± 0.11	1.32 ± 0.45	5.09 ± 0.24	1.36 ± 0.11
11c	**0.38 ± 0.08**	**0.74 ± 0.10**	**1.41 ± 0.15**	**0.93 ± 0.23**
11d	0.50 ± 0.08	1.31 ± 0.27	2.19 ± 0.08	**1.08 ± 0.20**
11e	0.74 ± 0.10	1.35 ± 0.11	3.16 ± 0.09	1.86 ± 0.21
11g	0.79 ± 0.12	1.16 ± 0.30	1.98 ± 0.08	1.28 ± 0.11
11h	0.58 ± 0.09	**0.76 ± 0.04**	1.97 ± 0.15	**1.03 ± 0.11**
11i	**0.35 ± 0.08**	1.27 ± 0.42	**1.27 ± 0.06**	**0.93 ± 0.01**
11j	1.01 ± 0.10	2.36 ± 1.21	**1.40 ± 0.12**	1.76 ± 0.51

[a] IC_{50} values (in μM) were calculated after 24 h (Jurkat) or 48 h (PC-3, T-47D, MB-468) of treatment with increasing concentrations (0.125−8 μM) of the indicated analogues. The average ± SD of two experiments performed in triplicate is shown. Lowest values for each cell line are in boldface.

respectively. Other analogues, **11b**, **11d**, **11e**, **11g**, and **11h**, also inhibited Jurkat cell proliferation with IC_{50} values below 1 μM (Table 1). We next evaluated the growth inhibitory activity of AdAr s against cell lines derived from solid tumors. We chose one prostate carcinoma cell line (PC-3) that has elevated basal IKK/NFκB activity[26] and two breast cancer cell lines, one estrogen-dependent (T-47D) and one estrogen-independent (MDA-MB-468). High IKK/NFκB activity has been reported to increase with tumor progression in breast carcinomas.[40−42] As shown in Table 1, **7** exhibited enhanced growth inhibitory activity against PC-3 and MDA-MB-468 cells compared to T-47D. As we observed in Jurkat T cells, most of the analogues with the exception of **24** were more effective than the parental compound **7** and they all showed IC_{50} values within the same range. Derivatives **11c** and **11h** were most active against PC-3

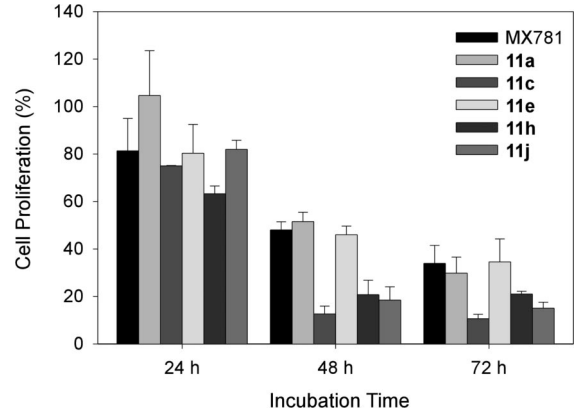

Figure 3. Time course of action of the AdAr s. MDA-MB-468 cells were incubated with 2 μM of the indicated AdAr s for 24, 48, or 72 h, when cell proliferation was measured by MTT. The experiment was repeated twice with triplicate time points, and the results of one representative experiment are shown.

cells, whereas compounds **11c**, **11d**, **11h**, and **11i** were highly active against MDA-MB-468 cells, with IC_{50} values about 2-fold lower than that obtained with **7**.

We then evaluated the time course of AdAr-mediated growth inhibitory activity, and Figure 3 illustrates the results obtained in MDA-MB-468 cells. As expected, the antiproliferative activity of the AdAr s significantly increased with the time of incubation and highly active derivatives (**11c**, **11h**) reached maximum activity after only 48 h of treatment. Less effective compounds exhibited increased growth inhibition with prolonged periods of exposure (72 h). Similar results were obtained with

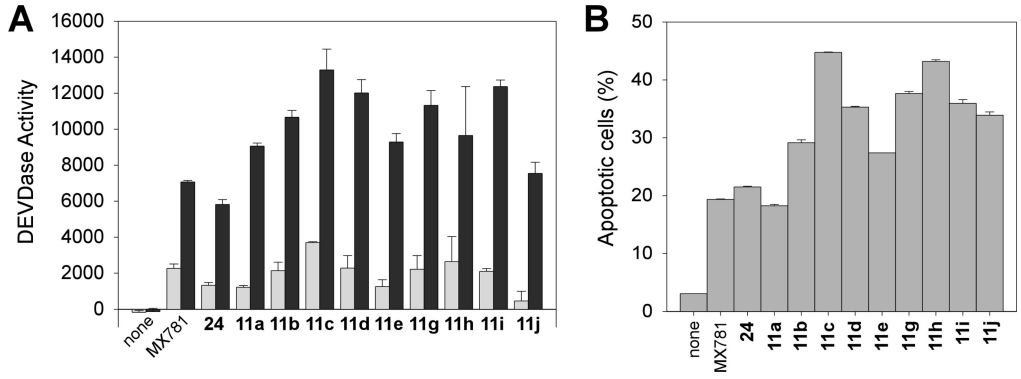

Figure 4. AdArs induce apoptosis in Jurkat T leukemia cells. (A) Induction of DEVDase activity by the MX781 analogues. Jurkat cells were incubated with 2 (light gray) or 4 (dark gray) μM of the indicated AdArs for 4 h, when DEVDase activity (arbitrary units) was evaluated as indicated in the Experimental Section. The experiment was performed twice with triplicates and the average ± standard deviation is shown. (B) Externalization of phosphatidylserine. Jurkat cells were incubated with 2 μM of the indicated compounds for 3 h, when cells were harvested and stained with annexin V-FITC and PI, followed by flow cytometry analysis. The experiment was performed three times with almost identical outcome, and the percentage of annexin V-positive/PI-negative cells of one representative experiment performed in duplicate is shown.

the rest of analogues, including **24**, which inhibited cell proliferation by ~40% after 72 h of treatment with 4 μM (not shown).

We previously reported that **7** and related RRMs rapidly induced caspase-dependent apoptosis in Jurkat T cells.[19,21] To evaluate the proapoptotic activity of the derivatives of **7**, we therefore analyzed the activation of caspases 3 and 7 by measuring the amount of DEVDase activity in cell extracts obtained from AdAr-stimulated Jurkat cells. All AdAr compounds induced significant levels of DEVDase activity in Jurkat T cells (Figure 4A) after 4 h of treatment. When tested at lower concentrations (1 μM), only the most active analogues (**11c**, **11d**, **11h**, and **11i**) induced substantial DEVDase activity (not shown). The enhanced caspase activation achieved by **11c** and **11i** paralleled the higher antiproliferative activity observed in Jurkat as well as in prostate and breast cancer cell lines (see Table 1). We then quantitated the induction of apoptosis at the cellular level by analyzing externalization of phosphatidylserine following staining with annexin V. Figure 4B illustrates that all analogues of **7** were at least as effective as the parent compound in increasing the percentage of annexin V-positive/PI-negative cells, which relates to early stages of apoptosis. As observed with DEVDase activity, compounds **11c** and **11h** induced the highest apoptotic rate when used at 2 μM.

Inhibition of IKK*β* by the Novel AdArs. We have shown that **7** is a strong inhibitor of IKK activity in vitro as well as in cell based assays.[26] A preliminary kinase profiler using recombinant kinases performed by Upstate demonstrated that **7** selectively inhibited IKKβ with an IC_{50} of 7 μM, with no effect on IKKα (data not shown). We therefore evaluated the inhibition of purified recombinant IKKβ expressed in baculovirus-infected Sf9 cells by the synthesized AdAr analogues. Figure 5 illustrates that 20 μM **7** inhibited IKKβ by ~65% in the presence of an ATP concentration corresponding to its K_m value. This inhibition is slightly lower but comparable to that originally observed in the Upstate's profile analysis, which might be likely due to the use of different peptide substrates, ATP concentrations, and/or enzyme preparations. With the exception of compounds **24** and **11j**, which showed partial inhibition of IKKβ, all other analogues **11a**−**i** elicited enhanced inhibition of the kinase compared to parent compound **7** and similar to that observed with two well characterized inhibitors of IKK (BMS345541 and SC-514) (Figure 5). In general, this increased inhibition of IKKβ parallels the growth inhibitory profile of the AdArs found in IKK-overexpressing cells (Jurkat, PC-3, and MDA-MB-468).

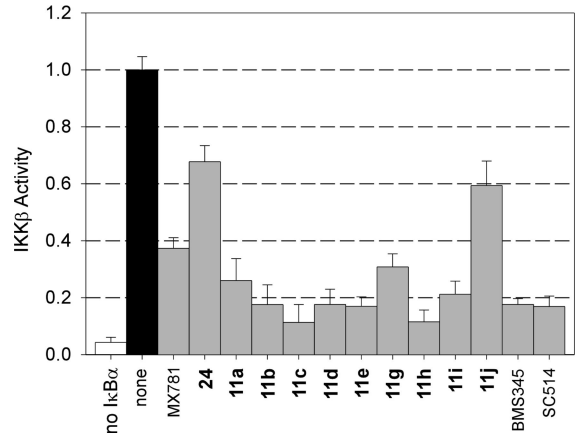

Figure 5. Effect of the MX781 analogues on recombinant IKKβ. Purified His-HA-IKKβ was incubated in the absence (none, black column) or in the presence of 20 μM of the indicated AdArs (gray columns). The white column (no IκBα) indicates basal IKK activity obtained in the absence of substrate. For comparison, the kinase was incubated with 10 μM BMS345541 (BMS345) or 20 μM SC-514. Kinase activity was determined after incubation at 30 °C for 30 min as specified in Experimental Section, and the ratio relative to control sample (none) was estimated. Shown here are the average ± SD of two to four experiments performed in triplicate.

Furthermore, the highest inhibition of IKKβ by **11c** and **11h** correlates well with the strongest induction of apoptosis observed in Jurkat cells (see Figure 4). More interestingly, compounds **11e** and **11i** exhibit improved anti-IKKβ and growth inhibitory activities and have lost their RAR-dependent transactivation function. These results clearly substantiate our assumption that modifications can be designed on the scaffold of **7** to increase antikinase activity while reducing or eliminating RAR-transactivation activity.

Discussion

Overwhelming evidence supports a critical role for IKK/NFκB activity in cancer progression, cell survival, and inhibition of TNFα-induced apoptosis.[27−29,40] Numerous inhibitors of IKK/NFκB activity have been described that act at different levels, including inhibitors that function upstream of the IKK complex, inhibitors of IKK activity, or inhibitors of NFκB nuclear functions.[43] Because IKKβ is the catalytic subunit essential for the activation of the classical NFκB pathway and is required for the reduced apoptosis rates observed in cancer cells,[44,45]

the development of IKKβ inhibitors is a promising strategy for novel cancer therapies, and several IKK inhibitors have indeed been described and are under clinical evaluation.[46] Some compounds inhibit IKKβ with an IC_{50} of 4−70 nM, but many of them are active at micromolar concentrations,[46] which is within the same range as **7** and analogues reported here. Using pharmacological and genetic inhibitors, we have established a correlation between inhibition of IKK/NFκB activity and induction of apoptosis in lung and prostate carcinoma cells. [26] Furthermore, RAR antagonist **7** and the RARγ/β agonist **8** inhibit in vitro the activity of IKK immunopurified from TNFα-stimulated HeLa cells,[26] and using recombinant IKKα and IKKβ proteins, we have now demonstrated that **7** is a selective inhibitor of IKKβ. Together, these data suggest that IKKβ is most likely involved in the anticancer activity mediated by **7** and validate IKKβ as an AdAr target. Although **7** inhibits recombinant IKKβ with an IC_{50} of 7 μM, it is very effective in cell-based assays, in which a 6 μM dose completely prevented activation of IKK by TNFα.[26] This contrasts with other typical kinase inhibitors such as AS602868, which normally require higher concentrations in cells to induce apoptosis than those required in vitro to inhibit purified kinase.[47] The reason for this discrepancy is unknown, but numerous factors such as cellular accumulation of the compound, its stability in culture medium, and most likely the targeting of alternative cell signaling molecules (see below) may certainly affect the anticancer activity of one compound in cell-based assays.

In contrast to the inhibition of IKK/NFκB signaling by **7**, it has recently been shown that **3** and its analogue **6** induce NFκB activity in prostate carcinoma cells, and this NFκB activation is necessary for apoptosis induction.[30,31] Compound **6** seems to activate IKKα in prostate carcinoma cells,[30] although the exact mechanism of IKK/NFκB activation by these AdArs remains unsolved. These observations were certainly unexpected; one could anticipate that retinoid agonists like **3** would inhibit NFκB transcriptional activity in a RAR-dependent manner. This effect has been observed with all-*trans*-retinoic acid (ATRA)[26] and could be explained by a ligand-dependent interaction of RARs with NFκB subunits, which would inhibit NFκB transcriptional activity in the absence of a direct effect on IKK activity. Besides IKK, a different target has been reported for **6** and related compounds, which bind the nuclear hormone receptor small heterodimer partner (SHP) and modulate SHP interaction with the Sin3A repressor.[48] Binding of **6** to SHP seems to mediate apoptosis, since SHP-deficient mouse embryo fibroblasts and breast carcinoma cells expressing reduced levels of SHP exhibit significantly lower degrees of apoptosis in response to this AdAr. In addition to IKK and SHP, some AdArs can also target certain protein phosphatases in vitro, including MKP-1 and the protein tyrosine phosphatases CD45 and SHP-2.[49,50] Inhibition of protein phosphatases has not yet been demonstrated in cell-based assays, and their relevance to AdAr anticancer activity needs to be addressed.

For the optimal development of novel RRMs with kinase inhibitory profiles with therapeutic potential, their RAR-dependent transcriptional activity should be reduced to a minimum because of the associated side effects of classical retinoids. In this regard, accumulating structural data on retinoid receptors have provided very efficient modulators (agonists, partial agonists, inverse agonists, and antagonists) of retinoid action and the current guidelines for optimizing their potency can be used in the reverse sense to minimize RAR binding and transactivation.[7,36,51,52] Whether protein kinases such as IKKβ are the main targets of RRM action or other receptors are also bound to mediate RRM-induced apoptosis, like SHP and protein phosphatases, the identification of these targets and their validation in cancer cells and in animal models will be absolutely critical for the optimization of RRMs/AdArs as effective anticancer drugs to evaluate in a clinical setting.

Here, we report on the biological activity of a series of analogues of **7** and their effect on recombinant IKKβ and cancer cell proliferation. Analogues were designed to have reduced RAR transactivation activity. The activities of the number of AdArs evaluated indicate that a hydroxy or an alkoxy group on the ring adjacent to the chalcone unit (**24**, **11a**−**j**) retain the activity of the parent system and are unable to activate RAR-mediated transcription. All compounds evaluated with the exception of **24** show reduced RAR binding, as evidenced by their significantly reduced antagonist activity. From the preliminary studies, the alkoxy group should be longer than a three-carbon atom, since the ethoxy derivative (**11a**) shows undesired RAR binding, although lower than the parent compound (MX781) **7**. Most analogues, including **11c** and the propargyl ether **11h** and **11c** afforded the strongest inhibition of IKKβ, concurring with the strongest induction of apoptosis in Jurkat cells and growth inhibitory activity against PC-3 and MDA-MB-468 cells. In general, there was a good correlation between the inhibition of recombinant IKKβ and the inhibition of cell growth in leukemia (Jurkat), prostate (PC-3), and breast (MDA-MB-468) cancer cells, all of which contain elevated basal IKK activity. These data suggest that IKKβ inhibition could mediate AdAr anticancer activity, although we do not rule out that other alternative mechanisms (targeting of SHP, protein phosphatases, other kinases) might be as critical for the anticancer activity of AdArs as blocking IKK/NFκB activity. Most importantly, the anticancer activity of these AdArs is completely independent of RAR transactivation activity (neither activation nor antagonism), thus confirming some of the design principles. The data reported here clearly demonstrate that we can design novel AdAr analogues lacking RAR activity that show improved anti-IKKβ and anticancer activities. Further verifying the inhibition of IKK signaling in cell-based assays and identifying novel targets of AdAr action will certainly facilitate clinical advancement of AdAr like molecules as alternative therapies for the chemoprevention and treatment of cancers.

Experimental Section

(*E*)-4-[3-(5-(Adamant-1-yl)-2-hydroxy-4-(2-methoxyethoxymethoxy)-phenyl)-3-oxoprop-1-en-1-yl]benzoic Acid 24. General Procedure for the Claisen−Schmidt Condensation. To a solution of 1-[5-(adamant-1-yl)-2-ethoxy-4-(2-methoxyethoxymethoxy)phenyl]ethan-2-one **19** (0.34 g, 0.91 mmol) and methyl 4-formylbenzoate **23** (0.18 g, 1.097 mmol) in MeOH (8.1 mL) was added a 1 M aqueous NaOH solution (5.4 mL), and the reaction mixture was heated to 70 °C for 18 h. After cooling to ambient temperature, the mixture was treated with a 10% aqueous HCl solution until acidic pH was attained and the mixture was extracted with AcOEt (3×). The combined organic layers were dried (Na_2SO_4), and the solvent was removed. The residue was purified by chromatography (silica gel, 98:2 CH_2Cl_2/MeOH) to afford 0.286 g (60%) of a yellow solid identified as (*E*)-4-[3-(5-adamant-1-yl)-2-hydroxy-4-(2-methoxyethoxymethoxy)phenyl)-3-oxoprop-1-en-1-yl]benzoic acid **24**. Mp 200 °C. Anal. ($C_{30}H_{34}O_7$): C, 71.13; H, 6.76. Found: C, 71.06; H, 7.16. ^{1}H NMR (400.13 MHz, $CDCl_3$): δ 8.15 (d, J = 8.2 Hz, 2H), 7.87 (d, J = 15.4 Hz, 1H), 7.73 (d, J = 8.3 Hz, 2H), 7.67 (s, 1H), 7.64 (d, J = 15.4 Hz, 1H), 6.69 (s, 1H), 5.36 (s, 2H), 3.9−3.8 (m, 2H), 3.6−3.5 (m, 2H), 3.39 (s, 3H), 2.1−2.0 (m, 9H), 1.8−1.7 (m, 6H) ppm. ^{13}C NMR (100.62 MHz, $CDCl_3$): δ 191.7 (s), 169.1 (s), 164.6 (s), 163.3 (s), 142.4 (s), 139.9 (d), 130.8 (d, 2×), 130.6 (s), 128.4 (d, 2×), 128.2 (d), 123.5 (s), 114.3 (s), 103.1 (d), 93.2

(t), 71.5 (t), 68.6 (t), 59.1 (q), 40.9 (t, 3×), 37.0 (t, 3×), 36.7 (s), 29.0 (d, 3×) ppm. MS (FAB^+): *m/z* (%) 507 (78), 506 (30), 392 (28), 391 (99), 307 (21), 167 (26), 155 (31), 154 (100). HRMS (FAB^+): calcd for $C_{30}H_{35}O_7$, 507.2383; found, 507.2384. IR (NaCl): ν 2910−2840 (s), 1690 (s), 1642 (s) cm^{-1}. UV (MeOH): λ_{max} 321 nm.

(*E*)-4-[3-(5-(Adamant-1-yl)-2-ethoxy-4-(2-methoxyethoxymethoxy)phenyl)-3-oxoprop-1-en-1-yl]benzoic Acid 11a. Following the general procedure for the Claisen−Schmidt condensation the reaction of 1-[5-(adamant-1-yl)-2-ethoxy-4-(2-methoxyethoxymethoxy)phenyl]ethan-2-one **22a** (0.14 g, 0.33 mmol), methyl 4-formylbenzoate **23** (0.066 g, 0.4 mmol), and a 1 M aqueous NaOH solution (2 mL) in MeOH (2 mL) afforded, after purification by chromatography (silica gel, 97:3 CH_2Cl_2/MeOH), 0.1 g (56%) of a yellow solid identified as (*E*)-4-[3-(5-(adamant-1-yl)-2-ethoxy-4-(2-methoxyethoxymethoxy)phenyl)-3-oxoprop-1-en-1-yl]benzoic acid **11a**. Mp: 182 °C. ^1H NMR (400.13 MHz, $CDCl_3$): δ 8.10 (d, J = 8.0 Hz, 2H), 7.77 (d, J = 15.5 Hz, 1H), 7.73 (s, 1H), 7.66 (d, J = 15.5 Hz, 1H), 7.65 (d, J = 8.5 Hz, 2H), 6.81 (s, 1H), 5.37 (s, 2H), 4.12 (t, J = 6.9 Hz, 2H), 3.9−3.8 (m, 2H), 3.6−3.5 (m, 2H), 3.40 (s, 3H), 2.1−2.0 (m, 9H), 1.8−1.7 (m, 6H), 1.44 (t, J = 7.0 Hz, 3H) ppm. ^{13}C NMR (100.62 MHz, $CDCl_3$): δ 190.2 (s), 168.0 (s), 161.3 (s), 158.3 (s), 140.9 (s), 139.1 (d), 131.5 (s), 130.7 (d, 2×), 130.2 (d), 130.0 (d), 129.8 (s), 128.0 (d, 2×), 121.4 (s), 99.8 (d), 93.2 (t), 71.5 (t), 67.9 (t), 64.6 (t), 59.0 (q), 40.9 (t, 3×), 37.1 (t, 3×), 36.7 (s), 29.0 (d, 3×), 14.9 (q) ppm. MS (FAB^+): *m/z* (%) 535 (89), 534 (18), 391 (12), 307 (26), 289 (15), 155 (32), 154 (100). HRMS (FAB^+): calcd for $C_{32}H_{39}O_7$, 535.2696; found, 535.2694. IR (NaCl): ν 2910−2840 (s), 1692 (s), 1608 (s) cm^{-1}. UV (MeOH): λ_{max} 313 nm.

(*E*)-4-[3-(5-Adamant-1-yl-4-(2-methoxyethoxymethoxy)-2-(prop-1-oxy)-phenyl)-3-oxoprop-1-en-1-yl]benzoic Acid 11b. Following the general procedure for the Claisen−Schmidt condensation the reaction of 1-[5-(adamant-1-yl)-4-(2-methoxyethoxymethoxy)-2-(prop-1-oxy)phenyl]ethan-2-one **22b** (0.077 g, 0.19 mmol), methyl 4-formylbenzoate **23** (0.038 g, 0.23 mmol), and a 1 M aqueous NaOH solution (1.1 mL) in MeOH (1.7 mL) afforded, after purification by chromatography (silica gel, 97:3 CH_2Cl_2/MeOH), 0.057 g (56%) of a yellow solid identified as (*E*)-4-[3-(5-(adamant-1-yl)-4-(2-methoxyethoxymethoxy)-2-(prop-1-oxy)phenyl)-3-oxoprop-1-en-1-yl]benzoic acid **11b**. Mp: 189 °C. Anal. ($C_{33}H_{40}O_7$), calcd: C, 72.24; H, 7.35. Found: C, 71.55; H, 7.31. ^1H NMR (400.13 MHz, $CDCl_3$): δ 8.11 (d, J = 8.3 Hz, 2H), 7.76 (d, J = 15.8 Hz, 1H), 7.73 (s, 1H), 7.68 (d, J = 15.8 Hz, 1H), 7.66 (d, J = 8.3 Hz, 2H), 6.81 (s, 1H), 5.38 (s, 2H), 4.01 (t, J = 6.4 Hz, 2H), 3.9−3.8 (m, 2H), 3.6−3.5 (m, 2H), 3.40 (s, 3H), 2.1−2.0 (s, 9H), 1.9−1.8 (m, 2H), 1.6−1.7 (s, 6H), 1.01 (t, J = 7.4 Hz, 3H) ppm. ^{13}C NMR (100.62 MHz, $CDCl_3$): δ 190.3 (s), 170.8 (s), 161.3 (s), 158.4 (s), 140.9 (s), 139.2 (d), 131.4 (s), 130.6 (d, 2×), 130.3 (d), 130.0 (d), 129.9 (s), 128.0 (d, 2×), 121.4 (s), 99.6 (d), 93.2 (t), 71.5 (t), 70.4 (t), 67.9 (t), 59.0 (q), 40.9 (t, 3×), 37.0 (t, 3×), 36.6 (s), 29.0 (d, 3×), 22.7 (t), 10.7 (q) ppm. MS (FAB^+): *m/z* (%) 549 (100), 548 (20), 391 (34), 307 (18), 289 (13), 167 (15), 165 (12), 155 (30), 154 (89), 151 (12). HRMS (FAB^+): calcd for $C_{33}H_{41}O_7$, 549.2852; found, 549.2851. IR (NaCl): ν 2910−2840 (s), 1691 (m), 1607 (m) cm^{-1}. UV (MeOH): λ_{max} 312 nm.

(*E*)-4-[3-(5-(Adamant-1-yl)-2-(but-1-oxy)-4-(2-methoxyethoxymethoxy)-phenyl)-3-oxoprop-1-en-1-yl]benzoic Acid 11c. Following the general procedure for the Claisen−Schmidt condensation the reaction of 1-[5-(adamant-1-yl)-2-(but-1-oxy)-4-(2-methoxyethoxymethoxy)phenyl]ethan-2-one **22c** (0.11 g, 0.30 mmol), methyl 4-formylbenzoate **23** (0.06 g, 0.36 mmol), and a 1 M aqueous NaOH solution (1.8 mL) in MeOH (2.6 mL) afforded, after purification by chromatography (silica gel, 95:5 CH_2Cl_2/MeOH), 0.091 g (58%) of a yellow solid identified as (*E*)-4-[3-(5-(adamant-1-yl)-2-(but-1-oxy)-4-(2-methoxyethoxymethoxy)phenyl)-3-oxoprop-1-en-1-yl-]benzoic acid **11c**. Mp: 156 °C. Anal. ($C_{34}H_{42}O_7$), calcd: C, 72.57; H, 7.52. Found: C, 72.09; H, 7.48. ^1H NMR (400.13 MHz, $CDCl_3$): δ 8.11 (d, J = 8.0 Hz, 2H), 7.76 (d, J = 16.0 Hz, 1H), 7.69 (s, 1H), 7.67 (d, J = 16.0 Hz, 1H), 7.65 (d, J = 8.0 Hz, 2H), 6.81 (s, 1H), 5.38 (s, 2H), 4.05 (t, J = 6.1 Hz, 2H), 3.9−3.8 (m, 2H), 3.6−3.5 (m, 2H), 3.40 (s, 3H), 2.1−2.0 (s, 9H), 1.8−1.7 (m, 8H), 1.45 (q, J = 7.5 Hz, 2H), 0.87 (t, J = 7.4 Hz, 3H) ppm. ^{13}C NMR (100.62 MHz, $CDCl_3$): δ 190.3 (s), 171.1 (s), 161.3 (s), 158.4 (s), 140.9 (s), 139.2 (d), 131.4 (s), 130.6 (d, 2×), 130.3 (d), 130.0 (s), 129.9 (d), 128.0 (d, 2×), 121.3 (s), 99.5 (d), 93.2 (t), 71.5 (t), 68.5 (t), 67.9 (t), 59.0 (q), 40.8 (t, 3×), 37.0 (t, 3×), 36.6 (s), 31.41 (t), 29.0 (d, 3×), 19.5 (t), 13.4 (q) ppm. MS (FAB^+): *m/z* (%) 563 (10), 562 (28), 486 (15), 473 (21), 175 (14), 89 (100). HRMS (FAB^+): calcd for $C_{34}H_{42}O_7$, 562.2931; found, 562.2935. IR (NaCl): ν 2910−2840 (s), 1718 (m), 1691 (m), 1607 (s) cm^{-1}. UV (MeOH): λ_{max} 309 nm.

(*E*)-4-[3-(5-(Adamant-1-yl)-4-(2-methoxyethoxymethoxy)-2-(pentyl-1-oxy)phenyl)-3-oxoprop-1-en-1-yl]benzoic Acid 11d. Following the general procedure for the Claisen−Schmidt condensation the reaction of 1-[5-(adamant-1-yl)-4-(2-methoxyethoxymethoxy)-2-(pentyl-1-oxy)phenyl]ethan-2-one **22d** (0.13 g, 0.29 mmol), methyl 4-formylbenzoate **23** (0.057 g, 0.35 mmol), and a 1 M aqueous NaOH solution (1.7 mL) in MeOH (2.6 mL) afforded, after purification by chromatography (silica gel, 97:3 CH_2Cl_2/MeOH), 0.058 g (35%) of a yellow solid identified as (*E*)-4-[3-(5-(adamant-1-yl)-4-(2-methoxyethoxymethoxy)-2-(pentyl-1-oxy)phenyl]-3-oxoprop-1-en-1-yl]benzoic acid **11d**. Mp: 149 °C. Anal. ($C_{35}H_{44}O_7$), calcd: C, 72.89; H, 7.69. Found: C, 72.87; H, 7.73. ^1H NMR (400.13 MHz, $CDCl_3$): δ 8.11 (d, J = 8.0 Hz, 2H), 7.75 (d, J = 15.8 Hz, 1H), 7.73 (s, 1H), 7.68 (d, J = 15.8 Hz, 1H), 7.65 (d, J = 8.0 Hz, 2H), 6.80 (s, 1H), 5.38 (s, 2H), 4.04 (t, J = 6.1 Hz, 2H), 3.9−3.8 (m, 2H), 3.6−3.5 (m, 2H), 3.40 (s, 3H), 2.1−2.0 (s, 9H), 1.9−1.8 (m, 2H), 1.8−1.7 (s, 6H), 1.5−1.4 (m, 2H), 1.3−1.2 (m, 2H), 0.79 (t, J = 7.2 Hz, 3H) ppm. ^{13}C NMR (100.62 MHz, $CDCl_3$): δ 190.3 (s), 171.1 (s), 161.3 (s), 158.4 (s), 140.9 (s), 139.2 (d), 131.4 (s), 130.6 (d), 130.3 (d), 130.1 (s), 130.0 (d, 2×), 128.0 (d, 2×), 121.3 (s), 99.5 (d), 93.2 (t), 71.5 (t), 68.9 (t), 67.9 (t), 59.0 (q), 40.9 (t, 3×), 37.0 (t, 3×), 36.6 (s), 29.2 (t), 29.0 (d, 3×), 28.4 (t), 22.4 (t), 13.8 (q) ppm. MS (FAB^+): *m/z* (%) 577 (100), 576 (20), 393 (12), 307 (24), 289 (14), 263 (15), 165 (12), 155 (32), 154 (95). HRMS (FAB^+): calcd for $C_{35}H_{45}O_7$, 577.3165; found, 577.3180. IR (NaCl): ν 2910−2840 (s), 1719 (m), 1692 (m), 1607 (s) cm^{-1}. UV (MeOH): λ_{max} 311 nm.

(*E*)-4-[3-(5-(Adamant-1-yl)-2-(hexyl-1-oxy)-4-(2-methoxyethoxymethoxy)phenyl)-3-oxoprop-1-en-1-yl]benzoic Acid 11e. Following the general procedure for the Claisen−Schmidt condensation the reaction of 1-[5-(adamant-1-yl)-2-(hexyl-1-oxy)-4-(2-methoxyethoxymethoxy)phenyl]ethan-2-one **22e** (0.11 g, 0.24 mmol), methyl 4-formylbenzoate **23** (0.048 g, 0.29 mmol), and a 1 M aqueous NaOH solution (1.4 mL) in MeOH (2.6 mL) afforded, after purification by chromatography (silica gel, 97:3 CH_2Cl_2/MeOH), 0.031 g (22%) of a yellow solid identified as (*E*)-4-[3-(5-(adamant-1-yl)-2-(hexyl-1-oxy)-4-(2-methoxyethoxymethoxy)phenyl)-3-oxoprop-1-en-1-yl]benzoic acid **11e**. Mp: 131 °C. Anal. ($C_{36}H_{46}O_7$), calcd: C, 73.19; H, 7.85. Found: C, 72.88; H, 7.75. ^1H NMR (400.13 MHz, $CDCl_3$): δ 8.11 (d, J = 8.8 Hz, 2H), 7.75 (d, J = 16.0 Hz, 1H), 7.73 (s, 1H), 7.69 (d, J = 16.0 Hz, 1H), 7.66 (d, J = 8.0 Hz, 2H), 6.80 (s, 1H), 5.38 (s, 2H), 4.04 (t, J = 6.6 Hz, 2H), 3.9−3.8 (m, 2H), 3.6−3.5 (m, 2H), 3.40 (s, 3H), 2.1−2.0 (s, 9H), 1.9−1.8 (m, 4H), 1.8−1.7 (s, 6H), 1.5−1.4 (m, 2H), 1.2−1.1 (m, 2H), 0.79 (t, J = 7.4 Hz, 3H) ppm. ^{13}C NMR (100.62 MHz, $CDCl_3$): δ 190.3 (s), 170.8 (s), 161.3 (s), 158.4 (s), 140.9 (s), 139.1 (d), 131.4 (s), 130.6 (d, 2×), 130.3 (d), 130.0 (d), 129.9 (s), 128.0 (d, 2×), 121.3 (s), 99.5 (d), 93.2 (t), 71.5 (t), 68.9 (t), 67.9 (t), 59.0 (q), 40.8 (t, 3×), 37.0 (t, 3×), 36.6 (s), 31.5 (t), 29.4 (t), 29.0 (d, 3×), 26.0 (t), 22.5 (t), 13.9 (q) ppm. MS (FAB^+): *m/z* (%) 591 (100), 590 (23), 307 (32), 289 (16), 155 (29), 154 (95). HRMS (FAB^+): calcd for $C_{36}H_{47}O_7$, 591.3322; found, 591.3306. IR (NaCl): ν 2910−2840 (s), 1716 (m), 1692 (m), 1650 (m), 1607 (s) cm^{-1}. UV (MeOH): λ_{max} 288 nm.

(*E*)-4-[3-(5-(Adamant-1-yl)-4-(2-methoxyethoxymethoxy)-2-(prop-2-en-1-oxy)phenyl)-3-oxoprop-1-en-1-yl]benzoic Acid 11g. Following the general procedure for the Claisen−Schmidt condensation the reaction of 1-[5-(adamant-1-yl)-4-(2-methoxyethoxymethoxy)-2-(prop-2-en-1-oxy)phenyl]ethan-2-one **22g** (0.086 g, 0.21 mmol), methyl 4-formylbenzoate **23** (0.041 g, 0.25 mmol), and a 1 M

aqueous NaOH solution (1.2 mL) in MeOH (1.8 mL) afforded, after purification by chromatography (silica gel, 97:3 CH_2Cl_2/MeOH), 0.064 g (57%) of a yellow solid identified as (*E*)-4-[3-(5-(adamant-1-yl)-4-(2-methoxyethoxymethoxy)-2-(prop-2-en-1-oxy)phenyl)-3-oxoprop-1-en-1-yl]benzoic acid **11g**. Mp: 182 °C. Anal. ($C_{33}H_{38}O_7$), calcd: C, 72.51; H, 7.01. Found: C, 72.40; H, 7.02. ^{1}H NMR (400.13 MHz, $CDCl_3$): δ 8.11 (d, J = 8.2 Hz, 2H), 7.75 (d, J = 15.8 Hz, 1H), 7.72 (s, 1H), 7.69 (d, J = 15.8 Hz, 1H), 7.66 (d, J = 8.2 Hz, 2H), 6.84 (s, 1H), 6.05 (tdd, J = 15.8, 10.3, 5.3 Hz, 1H), 5.44 (dd, J = 15.8, 1.4 Hz, 1H), 5.38 (s, 2H), 5.27 (dd, J = 10.3, 1.4 Hz, 1H), 4.6−4.5 (m, 2H), 3.9−3.8 (m, 2H), 3.6−3.5 (m, 2H), 3.40 (s, 3H), 2.1−2.0 (m, 9H), 1.8−1.7 (m, 6H) ppm. ^{13}C NMR (100.62 MHz, $CDCl_3$): δ 190.3 (s), 171.1 (s), 161.2 (s), 157.7 (s), 140.8 (s), 139.4 (d), 132.5 (d, 2×), 131.8 (s), 130.6 (d), 130.0 (d), 129.9 (s), 129.9 (d), 128.1 (d, 2×), 121.6 (s), 118.2 (t), 100.0 (d), 93.2 (t), 71.5 (t), 69.6 (t), 67.8 (t), 59.0 (q), 40.8 (t, 3×), 37.0 (t, 3×), 36.6 (s), 29.0 (d, 3×) ppm. MS (FAB^+): *m*/*z* (%) 547 (98), 546 (19), 307 (27), 289 (15), 175 (15), 155 (31), 154 (100), 151 (12). HRMS (FAB^+): calcd for $C_{33}H_{39}O_7$, 547.2696; found, 547.2691. IR (NaCl): ν 2910−2850 (s), 1717 (m), 1691 (s), 1607 (s) cm^{-1}. UV (MeOH): λ_{max} 314 nm.

(*E*)-4-[3-(5-(Adamant-1-yl)-4-(2-methoxyethoxymethoxy)-2-(prop-2-yn-1-oxy)phenyl)-3-oxoprop-1-en-1-yl]benzoic Acid 11h. Following the general procedure for the Claisen−Schmidt condensation the reaction of 1-[5-(adamant-1-yl)-4-(2-methoxyethoxymethoxy)-2-(prop-2-yn-1-oxy)phenyl]ethan-2-one **22h** (0.068 g, 0.17 mmol), methyl 4-formylbenzoate **23** (0.032 g, 0.20 mmol), and a 1 M aqueous NaOH solution (1.0 mL) in MeOH (1.5 mL) afforded, after purification by chromatography (silica gel, 97:3 CH_2Cl_2/MeOH), 0.045 g (50%) of a yellow solid identified as (*E*)-4-[3-(5-(adamant-1-yl)-4-(2-methoxyethoxymethoxy)-2-(prop-2-yn-1-oxy)phenyl)-3-oxoprop-1-en-1-yl]benzoic acid **11h**. ^{1}H NMR (400.13 MHz, $CDCl_3$): δ 8.12 (d, J = 8.0 Hz, 2H), 7.75 (d, J = 15.6 Hz, 1H), 7.74 (s, 1H), 7.71 (d, J = 7.8 Hz, 2H), 7.69 (d, J = 15.6 Hz, 1H), 6.91 (s, 1H), 5.39 (s, 2H), 4.80 (s, 2H), 3.9−3.8 (m, 2H), 3.6−3.5 (m, 2H), 3.41 (s, 3H), 2.57 (s, 1H), 2.1−2.0 (m, 9H), 1.8−1.7 (m, 6H) ppm. ^{13}C NMR (100.62 MHz, $CDCl_3$): δ 190.0 (s), 170.8 (s), 161.0 (s), 156.5 (s), 140.8 (s), 139.9 (d), 132.7 (s), 130.6 (d, 2×), 130.0 (d), 129.9 (s), 128.2 (d, 2×), 122.0 (s), 100.6 (d), 93.4 (t), 78.0 (d), 76.1 (d), 71.5 (t), 67.9 (t), 59.0 (q), 56.8 (t), 40.8 (t, 3×), 37.0 (t, 3×), 36.7 (s), 29.0 (d, 3×) ppm. MS (FAB^+): *m*/*z* (%) 545 (63), 544 (10), 307 (33), 289 (17), 155 (31), 154 (100), 151 (10). HRMS (FAB^+): calcd for $C_{33}H_{37}O_7$, 545.2539; found, 545.2547. IR (NaCl): ν 3246 (w), 2910−2850 (s), 1692 (s), 1606 (s) cm^{-1}. UV (MeOH): λ_{max} 313 nm.

(*E*)-4-[3-(5-(Adamant-1-yl)-4-(2-methoxyethoxymethoxy)-2-phenylmethoxy-phenyl)-3-oxoprop-1-en-1-yl]benzoic Acid 11i. Following the general procedure for the Claisen−Schmidt condensation the reaction of 1-[5-(adamant-1-yl)-4-(2-methoxyethoxymethoxy)-2-phenylmethoxyphenyl]ethan-2-one **22i** (0.13 g, 0.28 mmol), methyl 4-formylbenzoate **23** (0.094 g, 0.56 mmol), and a 1 M aqueous NaOH solution (1.6 mL) in MeOH (2.5 mL) afforded, after purification by chromatography (silica gel, 95:5 CH_2Cl_2/MeOH), 0.078 g (47%) of a yellow solid identified as (*E*)-4-[3-(5-(adamant-1-yl)-4-(2-methoxyethoxymethoxy)-2-phenylmethoxy-phenyl)-3-oxoprop-1-en-1-yl]benzoic acid **11i**. Mp: 167 °C. Anal. ($C_{37}H_{40}O_7$), calcd: C, 74.37; H, 6.76. Found: C, 73.89; H, 6.81. ^{1}H NMR (400.13 MHz, $CDCl_3$): δ 7.97 (d, J = 8.1 Hz, 2H), 7.83 (s, 1H), 7.74 (d, J = 15.7 Hz, 1H), 7.64 (d, J = 15.7 Hz, 1H), 7.45 (d, J = 7.0 Hz, 2H), 7.38 (d, J = 6.8 Hz, 2H), 7.36 (d, J = 6.8 Hz, 2H), 7.33 (t, J = 7.6 Hz, 1H), 6.96 (s, 1H), 5.40 (s, 2H), 5.13 (s, 2H), 3.9−3.8 (m, 2H), 3.6−3.5 (m, 2H), 3.41 (s, 3H), 2.1−2.0 (m, 9H), 1.8−1.7 (m, 6H) ppm. ^{13}C NMR (100.62 MHz, $CDCl_3$): δ 189.6 (s), 171.0 (s), 161.4 (s), 158.1 (s), 140.8 (s), 139.5 (d), 136.0 (s), 131.9 (s), 130.5 (d, 2×), 130.3 (d), 130.2 (d), 129.7 (s), 128.8 (d, 2×), 128.4 (d), 128.1 (d, 2×), 128.0 (d, 2×), 121.2 (s), 99.9 (d), 93.3 (t), 71.5 (t), 71.1 (t), 67.9 (t), 59.1 (q), 40.8 (t, 3×), 37.0 (t, 3×), 36.7 (s), 31.5 (t), 29.0 (d, 3×) ppm. MS (FAB^+): *m*/*z* (%) 597 (32), 596 (9), 308 (11), 307 (41), 289 (18), 155 (31), 154 (100), 151 (9). HRMS (FAB^+): calcd for $C_{37}H_{41}O_7$, 597.2852; found, 597.2862. IR (NaCl): ν 2910−2840 (m), 1715 (m), 1691 (m), 1606 (s) cm^{-1}. UV (MeOH): λ_{max} 315 nm.

(*E*)-4-[3-(5-(Adamant-1-yl)-4-(2-methoxyethoxymethoxy)-2-(*E*)-3-phenylprop-2-en-1-oxy)phenyl)-3-oxoprop-1-en-1-yl]benzoic Acid 11j. Following the general procedure for the Claisen−Schmidt condensation the reaction of 1-[5-(adamant-1-yl)-4-(2-methoxyethoxymethoxy)-2-(*E*)-3-phenylprop-2-en-1-oxy)phenyl]ethan-2-one **22j** (0.13 g, 0.27 mmol), methyl 4-formylbenzoate **23** (0.053 g, 0.32 mmol), and a 1 M aqueous NaOH solution (1.6 mL) in MeOH (2.4 mL) afforded, after purification by chromatography (silica gel, 98:2 CH_2Cl_2/MeOH), 0.038 g (23%) of a yellow solid identified as (*E*)-4-[3-(5-(adamant-1-yl)-4-(2-methoxyethoxymethoxy)-2-(*E*)-3-phenylprop-2-en-1-oxy)phenyl)-3-oxoprop-1-en-1-yl]benzoic acid **11j**. ^{1}H NMR (400.13 MHz, $CDCl_3$): δ 8.10 (d, J = 8.1 Hz, 2H), 7.87 (d, J = 8.1 Hz, 2H), 7.82 (s, 1H), 7.78 (d, J = 8.1 Hz, 2H), 7.67 (d, J = 15.8 Hz, 1H), 7.59 (d, J = 8.2 Hz, 2H), 7.57 (d, J = 15.8 Hz, 1H), 6.89 (s, 1H), 6.75 (d, J = 16.0 Hz, 1H), 6.41 (td, J = 15.9, 5.7 Hz, 1H), 5.40 (s, 2H), 4.77 (d, J = 5.5 Hz, 2H), 3.9−3.8 (m, 2H), 3.6−3.5 (m, 2H), 3.38 (s, 3H), 2.1−2.0 (m, 9H), 1.8−1.7 (m, 6H) ppm. MS (FAB^+): *m*/*z* (%) 623 (14), 549 (11), 393 (17), 392 (26), 391 (87), 369 (17), 330 (14), 322 (13), 307 (13), 279 (18), 221 (14), 207 (13), 203 (20), 191 (10). HRMS (FAB^+): calcd for $C_{39}H_{43}O_7$, 623.3009; found, 623.2996. IR (NaCl): ν 2910−2840 (s), 1718 (s), 1605 (s) cm^{-1}. UV (MeOH): λ_{max} 311 nm.

Cell Proliferation Assays. All cancer cell lines were obtained from ATCC and grown according to ATCC's suggestions. AdArs were prepared in DMSO as 4 mM stock solutions and diluted in basic DMEM as 20× dilutions. Cell proliferation assays were performed in 96-well plates. PC-3 cells, T-47D, and MDA-MB-468 (5000 cells per well) were seeded in complete growing medium the day before treatment and allowed to attach. Medium was changed to 0.5% FBS containing medium just before AdAr exposure. Jurkat T cells (10 000 cells per well) were resuspended (10^5 cells/mL) in RPMI supplemented with 0.5% FBS and seeded in 96-well plates immediately before AdAr treatment. Cells were treated with increasing concentrations of the AdArs, and when indicated, an amount of 10 μL of a 5 mg/mL 3-[4,5-dimethylthiazol-2-yl]-2,5-diphenyltetrazolium bromide (MTT) solution was added. After 4 h of incubation at 37 °C, an amount of 100 μL of 10% SDS in 10 mM HCl was added to solubilize the formazan crystals. The absorbance at 595 nm was measured in a Molecular Devices SpectraMax reader, and the background from wells with no cells was subtracted. The percentage of cell viability was calculated with respect to controls (100%), which were incubated with an equivalent amount of solvent DMSO (≤0.1% v/v). All experiments were performed at least twice with triplicate points. IC_{50} values were calculated using GraphPad Prism software.

Measurement of DEVDase Activity. To measure caspase activity, we adapted a fluorescence enzymatic assay[17] to 96-well plates. Jurkat T cells (40 000 cells per well, 10^6 cells/mL) in RPMI containing 0.5% FBS were seeded and immediately treated with AdArs. Alter 4 h of treatment, cells were lysed by adding 5× CE buffer (25 mM PIPES, pH 7, 25 mM KCl, 5 mM EGTA, 1 mM DTT, 10 μM cytochalasin B, 0.5% NP-40, and a mixture of protease inhibitors consisting of 1 mM PMSF, 1 μg/mL leupeptine, and 1 μg/mL aprotinin) followed by 30 min of incubation at 4 °C. Cell extracts were then diluted with 2× caspase buffer (50 mM HEPES, pH 7.4, 100 mM NaCl, 1 mM EDTA, 5 mM DTT, 0.1% CHAPS, and 10% sucrose) containing 100 μM Ac-DEVD-AFC (Enzyme System Products). Mixtures were incubated at 37 °C for 30 min, and the release of free AFC was measured every 2 min at 510 nm emission upon excitation at 390 nm, using a Victor2 microplate reader (Perkin-Elmer).

Staining with Annexin-FITC and PI. Jurkat cells (10^6 cells) were resuspended at a density of 500 000 cells/mL in medium containing 0.5% FBS and stimulated with 2 μM AdArs for 3 h. DMSO (0.1% v/v) was added to control cells. Following treatment, cells were washed with PBS and stained with annexin-V-FITC (BD Biosciences) and propidium iodine (PI) in binding buffer (10 mM Hepes, pH 7.4, 140 mM NaCl, 2.5 mM $CaCl_2$) during 15 min at room temperature and protected from light. Cells were subsequently

analyzed by flow cytometry (FACS Calibur) for apoptosis (FITC) and viability (PI).

RAR/RXR Transactivation Profiling. Gal4-LBD fusion proteins contain residues 1−147 encoding the DNA binding domain of Gal4 fused to the LBDs of the retinoid receptors: hRARα (residues 156−462), hRARβ (residues 149−448), hRARγ (residues 158−454), and mRXRα (residues 218−467). CV-1 cells (20 000 cells per well) were transfected in 96-well plates with 10 ng of each of the Gal4-LBD expression vectors together with 100 ng of UAS-luciferase reporter and 25 ng of β-galactosidase expression vector (pCH110) using Superfect transfection reagent. Sixteen hours after transfection, the medium was removed and fresh medium containing 5% charcoal-treated FBS was added, followed by AdAr stimulation for 6 h (20 h with RARγ). Cells were washed once with PBS, lysed, and assayed for luciferase and β-galactosidase activities using a Dual-Light chemiluminescent assay (Tropix).

IKKβ Expression, Purification, and Kinase Assays. $(His)_6$-HA-IKKβ was cloned into the pBAC-2 cP baculovirus expression vector (Novagen) and transfected into Sf9 cells using a BacVector-3000 DNA kit according to the manufacturer's instructions. Recombinant viruses were identified by PCR and subsequently purified and amplified to evaluate protein expression. Large scale protein expression and purification were carried out by infecting 1 L of Sf9 culture (2×10^6 cells/mL) with 25 mL of a high titer viral preparation. Sixty hours after infection, cells were harvested, washed with ice-cold PBS, and lysed in 10 mM Tris-HCl, pH 7.5, 150 mM NaCl, 1% NP-40 containing a mixture of protease and phosphatase inhibitors. $(His)_6$-HA-IKKβ was purified with 5 mL of ProBond resin (Invitrogen) under native conditions following the supplier's recommendations and dyalized against 50 mM Tris-HCl, pH 7.6, 270 mM sucrose, 150 mM NaCl, 1 mM benzamidine, 0.1 mM EGTA, 0.1% β-mercaptoethanol, 0.03% Brij-35, 0.2 mM PMSF.

To measure kinase activity, an amount of 100 ng of $(His)_6$-HA-IKKβ was diluted in a final volume of 25 μL with kinase buffer (8 mM MOPS, pH 7.0, 0.25 mM EDTA) containing 5 μg of GST-IκBα, 10 mM $MgCl_2$, 6.25 μM ATP, 2 μCi ^{32}P-γ-ATP, and 100 ng BSA. Reactions were incubated for 30 min at 30 °C, and an amount of 25 μL of 1% phosphoric acid was added to stop the reaction. Samples were transferred to a MultiScreen-PH (Millipore) filter plate, washed five times with 200 μL of 0.5% phosphoric acid, and air-dried. A total of 50 μL of OptiPhase Supermix scintillation liquid was added, and radioactivity was counted in a MicroBeta Trilux scintillation counter. Samples containing no IKKβ enzyme were used to subtract the background. When including inhibitors, these were added to an enzyme/substrate containing buffer mixture prior to the addition of an ATP/$MgCl_2$ cocktail. IKK inhibitors (BMS345541 and SC-514) were purchased from EMD Biosciences.

Acknowledgment. This work was supported by funds from the Spanish MEC (Grant SAF04-07131, FEDER to Á.R.d.L.), Xunta de Galicia (Grant PGIDIT05PXIC31403PN to Á.R.d.L.), and NIH (Grant CA55681 to F.J.P.). We thank Ming Zhao for technical assistance and Sandy Marsh for secretarial support.

Supporting Information Available: Additional details on experimental procedures and analytical and spectral characterization data for compounds **14**−**22**. This material is available free of charge via the Internet at http://pubs.acs.org.

References

(1) Hong, W. K.; Itri, L. M. Retinoids and Human Cancer. In *The Retinoids: Biology, Chemistry and Medicine*, 2nd ed.; Sporn, M. B., Roberts, A. B., Goodman, D. S., Eds.; Raven Press: New York, 1994; pp 597−630.

(2) Hong, W. K.; Sporn, M. B. Recent advances in chemoprevention of cancer. *Science* **1997**, *278*, 1073–1077.

(3) Liby, K. T.; Yore, M. M.; Sporn, M. B. Triterpenoids and rexinoids as multifunctional agents for the prevention and treatment of cancer. *Nat. Rev. Cancer* **2007**, *7*, 357–369.

(4) Laudet, V.; Gronemeyer, H. *The Nuclear Receptor Facts Book*; Academic Press: San Diego, CA, 2002.

(5) Germain, P.; Chambon, P.; Eichele, G.; Evans, R. M.; Lazar, M. A.; Leid, M.; de Lera, A. R.; Lotan, R.; Mangelsdorf, D. J.; Gronemeyer, H. The pharmacology and classification of the nuclear receptor superfamily. Retinoic acid receptors (RARs). *Pharmacol. Rev.* **2006**, *58*, 712–725.

(6) Germain, P.; Chambon, P.; Eichele, G.; Evans, R. M.; Lazar, M. A.; Leid, M.; de Lera, A. R.; Lotan, R.; Mangelsdorf, D. J.; Gronemeyer, H. The pharmacology and classification of the nuclear receptor superfamily. Retinoid x receptors (RXRs). *Pharmacol. Rev.* **2006**, *58*, 760–772.

(7) de Lera, A. R.; Bourguet, W.; Altucci, L.; Gronemeyer, H. Design of selective nuclear receptor modulators: RAR and RXR as a case study. *Nat. Rev. Drug Discovery* **2007**, *6*, 811–820.

(8) Germain, P.; Kammerer, S.; Perez, E.; Peluso-Iltis, C.; Tortolani, D.; Zusi, F. C.; Starrett, J.; Lapointe, P.; Daris, J. P.; Marinier, A.; de Lera, A. R.; Rochel, N.; Gronemeyer, H. Rational design of RAR-selective ligands revealed by RARbeta crystal stucture. *EMBO Rep.* **2004**, *5*, 877–882.

(9) Altucci, L.; Leibowitz, M. D.; Ogilvie, K. M.; de Lera, A. R.; Gronemeyer, H. RAR and RXR modulation in cancer and metabolic disease. *Nat. Rev. Drug Discovery* **2007**, *6*, 793–810.

(10) Altucci, L.; Gronemeyer, H. The promise of retinoids to fight against cancer. *Nat. Rev. Cancer* **2001**, *1*, 181–193.

(11) Piedrafita, F. J.; Ortiz, M. A. Mechanism of action and therapeutic potential of novel adamantyl retinoid-related molecules. *Curr. Cancer Ther. Rev.* **2006**, *2*, 185–198.

(12) Dawson, M. I.; Hobbs, P. D.; Peterson, V. J.; Leid, M.; Lange, C. W.; Feng, K. C.; Chen, G.; Gu, J.; Li, H.; Kolluri, S. K.; Zhang, X.; Zhang, Y.; Fontana, J. A. Apoptosis induction in cancer cells by a novel analogue of 6-[3-(1-adamantyl)-4-hydroxyphenyl]-2-naphthalenecarboxylic acid lacking retinoid receptor transcriptional activation activity. *Cancer Res.* **2001**, *61*, 4723–4730.

(13) Zhang, Y.; Dawson, M. I.; Mohammad, R.; Rishi, A. K.; Farhana, L.; Feng, K. C.; Leid, M.; Peterson, V.; Zhang, X. K.; Edelstein, M.; Eilander, D.; Biggar, S.; Wall, N.; Reichert, U.; Fontana, J. A. Induction of apoptosis of human B-CLL and ALL cells by a novel retinoid and its nonretinoidal analog. *Blood* **2002**, *100*, 2917–2925.

(14) Dawson, M. I.; Harris, D. L.; Liu, G.; Hobbs, P. D.; Lange, C. W.; Jong, L.; Bruey-Sedano, N.; James, S. Y.; Zhang, X. K.; Peterson, V. J.; Leid, M.; Farhana, L.; Rishi, A. K.; Fontana, J. A. Antagonist analogue of 6-[3′-(1-adamantyl)-4′-hydroxyphenyl]-2-naphthalenecarboxylic acid (AHPN) family of apoptosis inducers that effectively blocks AHPN-induced apoptosis but not cell-cycle arrest. *J. Med. Chem.* **2004**, *47*, 3518–3536.

(15) Adachi, H.; Adams, A.; Hughes, F. M.; Zhang, J.; Cidlowski, J. A.; Jetten, A. M. Induction of apoptosis by the novel retinoid AHPN in human T-cell lymphoma cells involves caspase-dependent and independent pathways. *Cell Death Differ.* **1998**, *5*, 973–983.

(16) Zang, Y.; Beard, R. L.; Chandraratna, R. A.; Kang, J. X. Evidence of a lysosomal pathway for apoptosis induced by the synthetic retinoid CD437 in human leukemia HL-60 cells. *Cell Death Differ.* **2001**, *8*, 477–485.

(17) Lopez-Hernandez, F. J.; Ortiz, M. A.; Bayon, Y.; Piedrafita, F. J. Retinoid-related molecules require caspase 9 for the effective release of Smac and the rapid induction of apoptosis. *Cell Death Differ.* **2004**, *11*, 154–164.

(18) Marchetti, P.; Zamzami, N.; Joseph, B.; Schraen-Maschke, S.; Mereau-Richard, C.; Costantini, P.; Metivier, D.; Susin, S. A.; Kroemer, G.; Formstecher, P. The novel retinoid 6-[3-(1-adamantyl)-4-hydroxyphenyl]-2-naphtalene carboxylic acid can trigger apoptosis through a mitochondrial pathway independent of the nucleus. *Cancer Res.* **1999**, *59*, 6257–6266.

(19) Lopez-Hernandez, F. J.; Ortiz, M. A.; Bayon, Y.; Piedrafita, F. J. Z-FA-fmk inhibits effector caspases but not initiator caspases 8 and 10, and demonstrates that novel anticancer retinoid-related molecules induce apoptosis via the intrinsic pathway. *Mol. Cancer Ther.* **2003**, *2*, 255–263.

(20) Chun, K. H.; Pfahl, M.; Lotan, R. Induction of apoptosis by the synthetic retinoid MX3350-1 through extrinsic and intrinsic pathways in head and neck squamous carcinoma cells. *Oncogene* **2005**, *24*, 3669–3677.

(21) Ortiz, M. A.; Lopez-Hernandez, F. J.; Bayon, Y.; Pfahl, M.; Piedrafita, F. J. Retinoid-related molecules induce cytochrome *c* release and apoptosis through activation of c-Jun NH(2)-terminal kinase/p38 mitogen-activated protein kinases. *Cancer Res.* **2001**, *61*, 8504–8512.

(22) Holmes, W. F.; Soprano, D. R.; Soprano, K. J. Elucidation of molecular events mediating induction of apoptosis by synthetic retinoids using a CD437-resistant ovarian carcinoma cell line. *J. Biol. Chem.* **2002**, *277*, 45408–45419.

(23) Zhang, Y.; Dawson, M. I.; Ning, Y.; Polin, L.; Parchment, R. E.; Corbett, T.; Mohammad, A. N.; Feng, K. C.; Farhana, L.; Rishi, A. K.; Hogge, D.; Leid, M.; Peterson, V. J.; Zhang, X. K.; Mohammad, R.;

Lu, J. S.; Willman, C.; VanBuren, E.; Biggar, S.; Edelstein, M.; Eilender, D.; Fontana, J. A. Induction of apoptosis in retinoid refractory acute myelogenous leukemia by a novel AHPN analog. *Blood* **2003**, *102*, 3743–3752.

(24) Zhang, Y.; Huang, Y.; Rishi, A. K.; Sheikh, M. S.; Shroot, B.; Reichert, U.; Dawson, M.; Poirer, G.; Fontana, J. A. Activation of the p38 and JNK/SAPK mitogen-activated protein kinase pathways during apoptosis is mediated by a novel retinoid. *Exp. Cell Res.* **1999**, *247*, 233–240.

(25) Garattini, E.; Parrella, E.; Diomede, L.; Gianni', M.; Kalac, Y.; Merlini, L.; Simoni, D.; Zanier, R.; Ferrara, F. F.; Chiarucci, I.; Carminati, P.; Terao, M.; Pisano, C. ST1926, a novel and orally active retinoid-related molecule inducing apoptosis in myeloid leukemia cells: modulation of intracellular calcium homeostasis. *Blood* **2004**, *103*, 194–207.

(26) Bayon, Y.; Ortiz, M. A.; Lopez-Hernandez, F. J.; Gao, F.; Karin, M.; Pfahl, M.; Piedrafita, F. J. Inhibition of IκB kinase by a new class of retinoid-related anticancer agents that induce apoptosis. *Mol. Cell. Biol.* **2003**, *23*, 1061–1074.

(27) Van Antwerp, D. J.; Martin, S. J.; Kafri, T.; Green, D. R.; Verma, I. M. Suppression of TNF-alpha-induced apoptosis by NF-kappaB. *Science* **1996**, *274*, 787–789.

(28) Wang, C. Y.; Mayo, M. W.; Baldwin, A. S. J. TNF- and cancer therapy-induced apoptosis: potentiation by inhibition of NF-kappaB. *Science* **1996**, *274*, 784–787.

(29) Beg, A. A.; Baltimore, D. An essential role for NFκB in preventing TNFα-induced cell death. *Science* **1996**, *274*, 782–784.

(30) Farhana, L.; Dawson, M. I.; Fontana, J. A. Apoptosis induction by a novel retinoid-related molecule requires nuclear factor-kappaB activation. *Cancer Res.* **2005**, *65*, 4909–4917.

(31) Jin, F.; Liu, X.; Zhou, Z.; Yue, P.; Lotan, R.; Khuri, F. R.; Chung, L. W.; Sun, S. Y. Activation of nuclear factor-kappaB contributes to induction of death receptors and apoptosis by the synthetic retinoid CD437 in DU145 human prostate cancer cells. *Cancer Res.* **2005**, *65*, 6354–6363.

(32) Charpentier, B.; Bernardon, J. M.; Eustache, J.; Millois, C.; Martin, B.; Michel, S.; Shroot, B. Synthesis, structure−affinity relationships, and biological activities of ligands binding to retinoic acid receptor subtypes. *J. Med. Chem.* **1995**, *38*, 4993–5006.

(33) Keedwell, R. G.; Zhao, Y.; Hammond, L. A.; Qin, S.; Tsang, K. Y.; Reitmair, A.; Molina, Y.; Okawa, Y.; Atangan, L. I.; Shurland, D. L.; Wen, K.; Wallace, D. M.; Bird, R.; Chandraratna, R. A.; Brown, G. A retinoid-related molecule that does not bind to classical retinoid receptors potently induces apoptosis in human prostate cancer cells through rapid caspase activation. *Cancer Res.* **2004**, *64*, 3302–3312.

(34) Karin, M.; Cao, Y.; Greten, F. R.; Li, Z. W. NF-kappaB in cancer: from innocent bystander to major culprit. *Nat. Rev. Cancer* **2002**, *2*, 301–310.

(35) Gronemeyer, H.; Gustafsson, J. A.; Laudet, V. Principles for modulation of the nuclear receptor superfamily. *Nat. Rev. Drug Discovery* **2004**, *3*, 950–964.

(36) Klaholz, B. P.; Mitschler, A.; Moras, D. Structural basis for isotype selectivity of the human retinoic acid nuclear receptor. *J. Mol. Biol.* **2000**, *302*, 155–170.

(37) Singh, C.; Gupta, N.; Puri, S. K. Synthesis of new 6-alkylvinyl/arylalkylvinyl substituted 1,2,4-trioxanes active against multidrug-resistant malaria in mice. *Bioorg. Med. Chem.* **2004**, *12*, 5553–5562.

(38) Bernard, A.; Bernardon, J.-M.; Delescluse, C.; Martin, B.; Lenoir, M.-C.; Maignan, J.; Charpentier, B.; Pilgrim, W. R.; Reichert, U.; Shroot, B. Identification of synthetic retinoids with selectivity for human nuclear retinoic acid receptor γ. *Biochem. Biophys. Res. Commun.* **1992**, *186*, 977–983.

(39) Germain, P.; Iyer, J.; Zechel, C.; Gronemeyer, H. Co-regulator recruitment and the mechanism of retinoic acid receptor synergy. *Nature* **2002**, *415*, 187–192.

(40) Nakshatri, H.; Bhat-Nakshatri, P.; Martin, D. A.; Goulet, R. J. J.; Sledge, G. W. J. Constitutive activation of NF-kappaB during progression of breast cancer to hormone-independent growth. *Mol. Cell. Biol.* **1997**, *17*, 3629–3639.

(41) Sovak, M. A.; Bellas, R. E.; Kim, D. W.; Zanieski, G. J.; Rogers, A. E.; Traish, A. M. Aberrant nuclear factor-kB/Rel expression and the pathogenesis of breast cancer. *J. Clin. Invest.* **1997**, *100*, 2952–2960.

(42) Biswas, D. K.; Cruz, A. P.; Gansberger, E.; Pardee, A. B. Epidermal growth factor-induced nuclear factor kappa B activation: a major pathway of cell-cycle progression in estrogen-receptor negative breast cancer cells. *Proc. Natl. Acad. Sci. U.S.A.* **2000**, *97*, 8542–8547.

(43) Gilmore, T. D.; Herscovitch, M. Inhibitors of NF-kappaB signaling: 785 and counting. *Oncogene* **2006**, *25*, 6887–6899.

(44) Li, Q.; Van Antwerp, D.; Mercurio, F.; Lee, K. F.; Verma, I. M. Severe liver degeneration in mice lacking the IkappaB kinase 2 gene. *Science* **1999**, *284*, 321–325.

(45) Li, Z. W.; Chu, W.; Hu, Y.; Delhase, M.; Deerinck, T.; Ellisman, M.; Johnson, R.; Karin, M. The IKKbeta subunit of IkappaB kinase (IKK) is essential for nuclear factor kappaB activation and prevention of apoptosis. *J. Exp. Med.* **1999**, *189*, 1839–1845.

(46) Karin, M.; Yamamoto, Y.; Wang, Q. M. The IKK NF-kappa B system: a treasure trove for drug development. *Nat. Rev. Drug Discovery* **2004**, *3*, 17–26.

(47) Frelin, C.; Imbert, V.; Griessinger, E.; Loubat, A.; Dreano, M.; Peyron, J. F. AS602868, a pharmacological inhibitor of IKK2, reveals the apoptotic potential of TNF-α in Jurkat leukemia cells. *Oncogene* **2003**, *22*, 8187–8194.

(48) Farhana, L.; Dawson, M. I.; Leid, M.; Wang, L.; Moore, D. D.; Liu, G.; Xia, Z.; Fontana, J. A. Adamantyl-substituted retinoid-related molecules bind small heterodimer partner and modulate the Sin3A repressor. *Cancer Res.* **2007**, *67*, 318–325.

(49) Pfahl, M.; Piedrafita, F. J. Retinoid targets for apoptosis induction. *Oncogene* **2003**, *22*, 9058–9062.

(50) Dawson, M. I.; Xia, Z.; Liu, G.; Fontana, J. A.; Farhana, L.; Patel, B. B.; Arumugarajah, S.; Bhuiyan, M.; Zhang, X. K.; Han, Y. H.; Stallcup, W. B.; Fukushi, J.; Mustelin, T.; Tautz, L.; Su, Y.; Harris, D. L.; Waleh, N.; Hobbs, P. D.; Jong, L.; Chao, W. R.; Schiff, L. J.; Sani, B. P. An adamantyl-substituted retinoid-derived molecule that inhibits cancer cell growth and angiogenesis by inducing apoptosis and binds to small heterodimer partner nuclear receptor: effects of modifying its carboxylate group on apoptosis, proliferation, and protein−tyrosine phosphatase activity. *J. Med. Chem.* **2007**, *50*, 2622–2639.

(51) Zusi, F. C.; Lorenzi, M. V.; Vivat-Hannah, V. Selective retinoids and rexinoids in cancer therapy and chemoprevention. *Drug Discovery Today* **2002**, *7*, 1165–1174.

(52) Dawson, M. I.; Zhang, X. K. Discovery and design of retinoic acid receptor and retinoid X receptor class- and subtype-selective synthetic analogues of all-*trans*-retinoic acid and 9-*cis*-retinoic acid. *Curr. Med. Chem.* **2002**, *9*, 623–637.

JM800285F